

## Materials Science inc. Nanomaterials &amp; Polymers

## Room Temperature-Sintering Conductive Ink Fabricated from Oleic-Modified Graphene for the Flexible Electronic Devices

Tam The Le,<sup>[a]</sup> Huy Hoang Tran Bui,<sup>[b]</sup> An Khang Phung Dinh,<sup>[c]</sup> Duc Vu Van,<sup>[d]</sup> Quang Dinh Ho,<sup>[a]</sup> Hoai An Nguyen Thi,<sup>[b]</sup> Du Hoa Nguyen,<sup>[a]</sup> and Duong Duc La<sup>\*[e]</sup>

Graphene, a novel 2D nanomaterial, has been intensively studied and utilized in many fields of applications. Graphene-based conductive ink has attracted many scientific researchers due to its flexibility, durability, and, most importantly, high electrical conductivity. However, the low dispensability and high curing temperature have hindered the use of graphene ink in many practical applications. In this work, graphene nanoplatelets (GNPs) were modified with oleic acid to improve dispensability. Then, the modified GNPs were employed as a major component in the conductive ink's formulation. The effects of the oleic acid, binder, and GNPs contents on the

conductivity of the prepared ink were studied. The results showed that at the ink's formulation of 0.75% binder and 6% GNPs (modified with 2.5% oleic acid), the lowest resistance with the value of 22  $\Omega$ .cm and sheet resistance of 7.56  $\Omega$  cm<sup>2</sup> was obtained. Remarkably, the high conductivity of the modified conductive ink on the substrate could also be observed after curing at room temperature, which is advantageous for practical application. The viscosity of the resultant conductive ink could also be adjusted by changing the amount of solvent in the ink's formulation for application of the ink in the pen, painting, or inkjet printing.

## Introduction

The flexible and low-cost electronic devices have attracted extensive attention from scientists and governments worldwide for innovative and future applications such as sensors, electronic displays, smart clothing, solar cells, and field-effect transistors.<sup>[1,5]</sup> One of the main driving forces for developing flexible and low-cost electronic devices is the fabrication of conductive ink.<sup>[6,7]</sup> To fabricate electronic devices and sensors, conductive ink could be facilely printed on sensitive and flexible substrates such as plastic, clothes, polymeric surfaces, and papers.<sup>[8–11]</sup> It is necessary to find appropriate ink formulations that can be processed by screen or inkjet printing to maintain high mechanical and electrical performance. Many conductive fillers have been successfully employed to formulate the conductive inks, including, but not limited to, metals, conductive polymers, carbon-based materials, and organic

metal complexes.<sup>[12,18]</sup> Among these, silver nanoparticles are considered as one of the most suitable fillers for the fabrication of conductive ink with high conductivity.<sup>[18,20]</sup> However, because of its high cost and electromigration property, silver has limited its application on a large scale. An alternative promising conducting filler in the conductive ink formulation is copper nanoparticles, which are cost-effective for industrial applications. However, the copper nanoparticles are easy to oxidize to form the copper oxides, increasing the curing temperature of the ink and reducing conductivity.<sup>[21,23]</sup> The copper-based conductive inks are also of poor thermal and chemical stability. Several carbon-based nanomaterials such as graphene and carbon nanotubes have been widely studied as fillers in the ink's formulations.<sup>[24,29]</sup> However, carbon-based materials have low dispensability in the ink's composition, which significantly hindered their applications. Thus, developing a new conductive ink formulation for flexible electronic devices and sensors is necessary.

Graphene, a 2D (2D) carbon nanomaterial with remarkable mechanical, electrical and thermal properties, have been widely used in a wide range of industrial applications including, but not limited to, support substrate for photocatalysis, supercapacitors, sensors, fillers, and light-emitting diodes.<sup>[27][30,35]</sup> Thanks to the excellent conductivity and transparency property, graphene could be employed as a main conductive component for the fabrication of printable ink.<sup>[36,39]</sup> The graphene ink could be patterned using two general processes of ink transfer and sintering. For example, Gao's group successfully fabricated graphene-based ink from pristine graphene, cyclohexanone, and ethyl cellulose using an ultrasonic CO<sub>2</sub>-based approach.<sup>[40]</sup> The prepared ink showed low sheet

[a] Dr. T. T. Le, Dr. Q. D. Ho, Prof. D. H. Nguyen  
Vinh University, 182 Le Duan, Vinh City 460000, Vietnam

[b] H. H. T. Bui, H. A. N. Thi  
Ha Huy Tap High school, 8 Phan Boi Chau Street, Vinh City 460000, Vietnam

[c] A. K. P. Dinh  
Phan Boi Chau Specialized High School, 119 Le Hong Phong Street, Vinh City 460000, Vietnam

[d] D. V. Van  
Applied Nano Technology Jsc, Xuan La, Tay Ho, Hanoi 100000, Vietnam

[e] Dr. D. D. La  
Institute of Chemistry and Materials, Hoang Sam road, Nghia Do, Hanoi 100000, Vietnam  
E-mail: duc.duong.la@gmail.com

Supporting information for this article is available on the WWW under <https://doi.org/10.1002/slct.202104249>

resistance of  $0.81 \pm 0.2 \text{ k}\Omega \text{ cm}^2$  after sintering at  $300^\circ\text{C}$  for 30 minutes. The flexible ink-printed substrate remained high conductivity even after 1000 folding cycles. However, the processing at high temperatures limited their application of flexible substrates such as PET. To enhance the dispensability of graphene in the ink's formulation, a modification pathway through non-covalent or covalent interaction is usually employed.<sup>[41]–[44]</sup> Most of the graphene modification aimed to improve the dispensability in the aqueous-based ink formulation. Thus, the quest of finding a graphene-based ink formulation with high stability and conductivity, even sintering at room temperature, is essential for applications in flexible electronic devices and sensors.

Herein, the pristine graphene nanoplatelets (GNPs) are modified with oleic acid and employed as a filler to formulate the conductive ink. The oleic-modified GNPs will be thoroughly characterized. The effects of the oleic acid modified GNPs, and binder contents on the conductivity of the prepared ink are investigated. Significantly, the effect of the sintering temperature of the ink on the conductivity is also discussed in detail.

Several examples of the practical application of the prepared ink are also illustrated.

## Results and discussion

The morphologies of the graphene nanoplatelets (GNPs) and the oleic-modified GNPs were observed using electron scanning microscopy, as shown in Figure 1. It can be seen that GNPs are of wrinkle and crumpled morphologies with a diameter in the range of micrometers (Figure 1a). The semi-transparent property to the electron beam of the SEM instrument demonstrates that the GNPs consist of a few layers of graphene.<sup>[35]</sup> After modification with oleic acid, the GNPs tend to stack to each other (Figure 1b). The modified GNPs are non-semi-transparent to the electron beam, which indicates that the GNPs' surface was uniformly covered by oleic acid. The purity of the graphene nanoplatelets was determined using EDX spectrum, which indicates that the GNPs have a purity of almost 100% (Figure S1). The AFM analysis shows that the

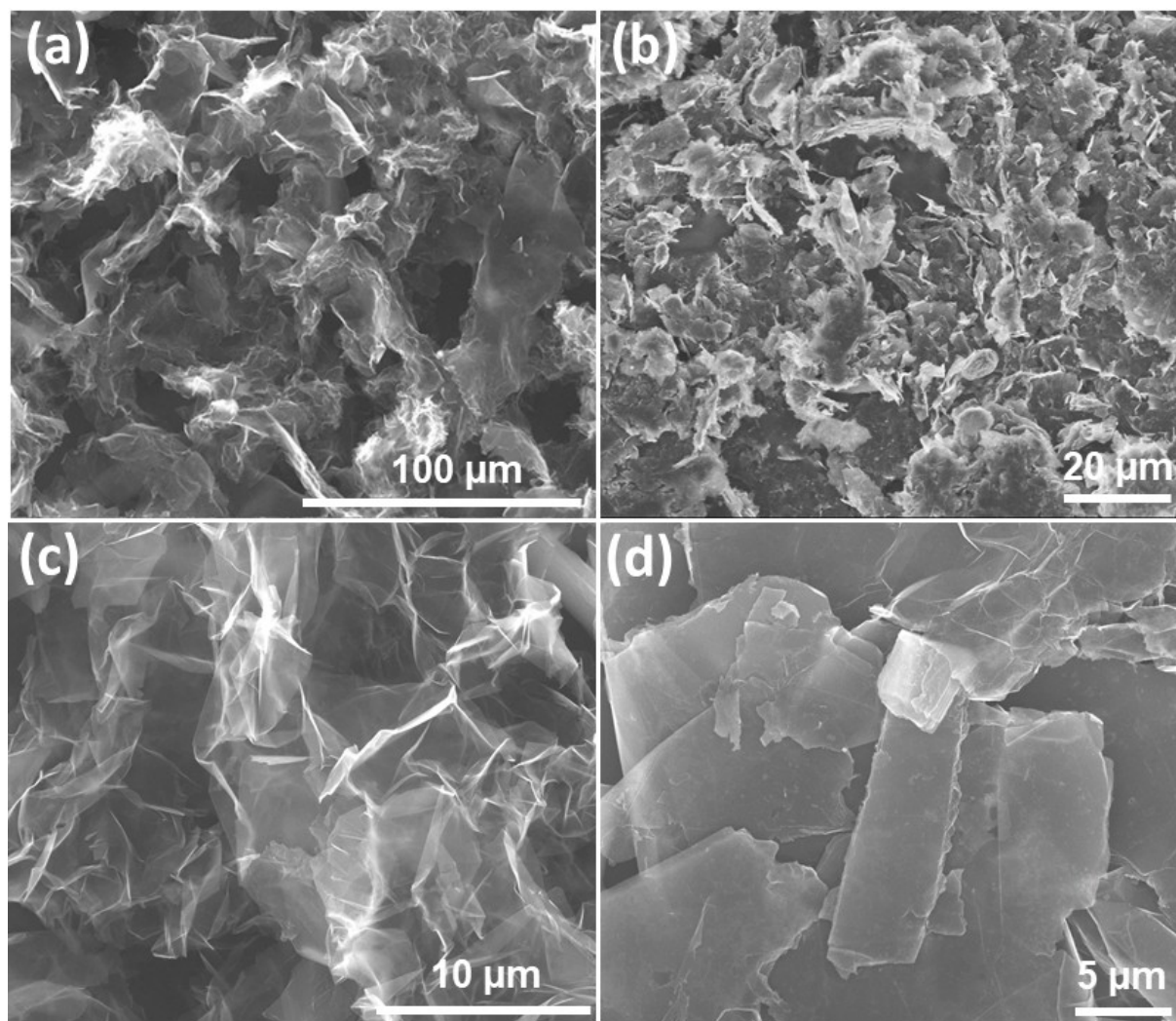


**Figure 1.** The SEM images of (a,c) the graphene nanoplatelets and (b,d) oleic-modified graphene nanoplatelets.

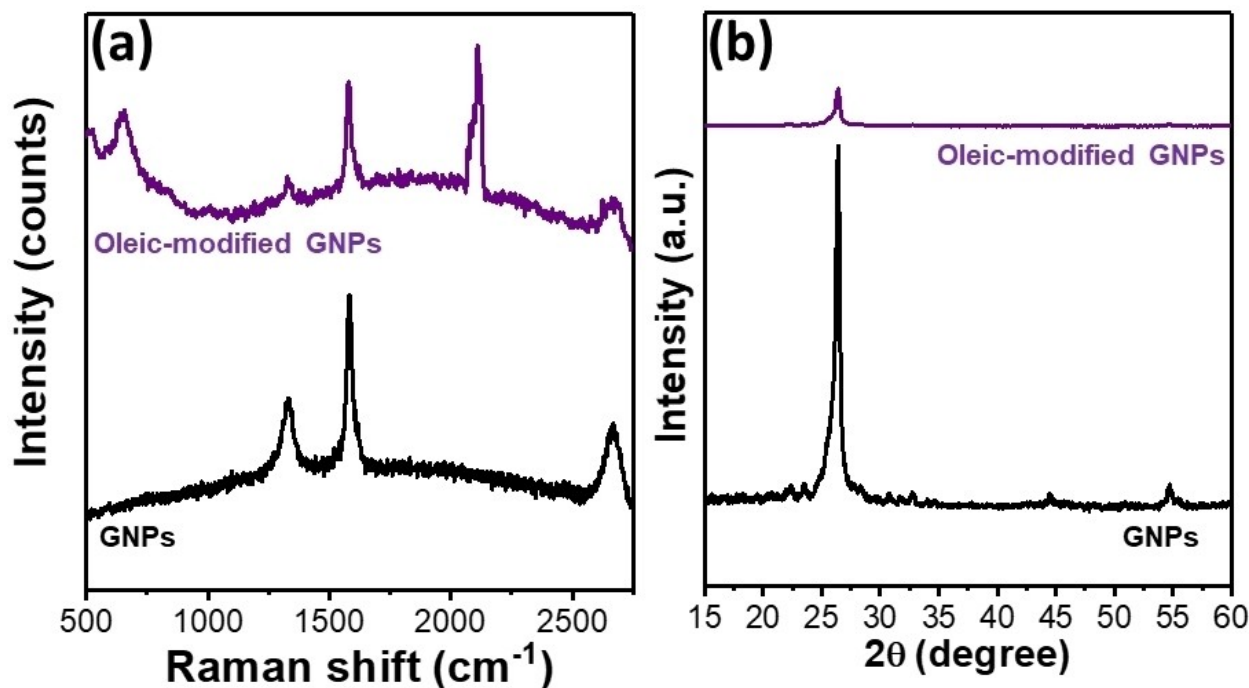


Figure 2. (a) Raman spectra and (b) XRD patterns of graphene nanoplatelets (black line) and oleic-modified graphene nanoplatelets (purple line).

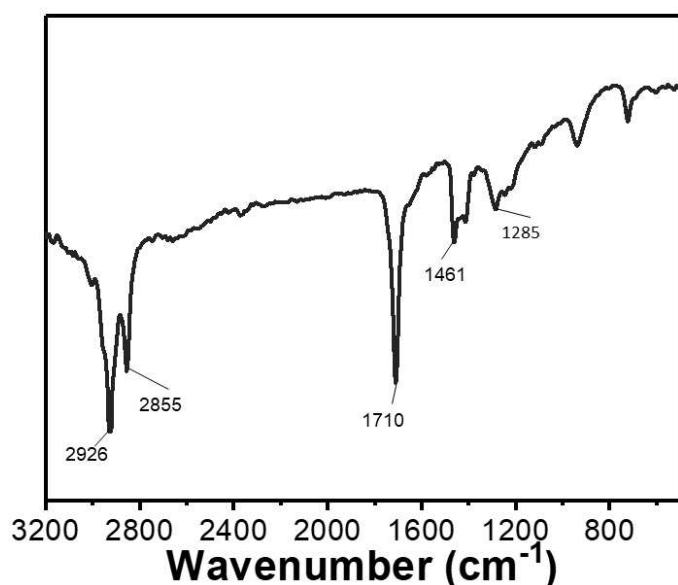


Figure 3. Fourier transforms infrared (FTIR) spectrum of the modified GNPs.

GNPs has the thickness of around 10 nm, which is equivalent to approximately 20 layers of graphene (Figure S2).

The chemical structure of the GNPs and the modified GNPs were studied using Raman spectroscopy, as shown in Figure 2a. The Raman spectrum of the GNPs has two characteristic peaks at 1336 (D band) and 1581  $\text{cm}^{-1}$  (G band), corresponding to the defects in carbon networks and  $\text{sp}^2$  bonding, respectively, of carbon elements. The D band peak's intensity is significantly lower than the G band peak, indicating that the obtained GNPs

have fewer defects and a lower oxidant degree. Moreover, the appearance of a peak at 2658  $\text{cm}^{-1}$  (assigned to the 2D band), with an intensity significantly lower than that of the G band, indicates that the GNPs are multilayered. The broad photoluminescent band in the Raman spectrum of the GNPs might be due to the amorphous nature of the graphene nanoplatelets. In the Raman spectrum of the oleic-modified GNPs, it can be seen that along with the presence of characteristic bands of GNPs, the CD-stretching vibrations at around 2100 and 2195  $\text{cm}^{-1}$  are assigned to the characteristic bands of the oleic acid. Figure 2b shows the XRD patterns of the GNPs and modified GNPs. The XRD pattern of the GNPs reveals a peak at 26.4°, which is characteristic of the graphitic nature of graphene materials. Interestingly, the intensity of the characteristic peaks in the XRD pattern of the modified GNPs at 26.4° significantly decreases after modifying the pristine GNPs with oleic acid. The decrease in the diffraction peak's intensity further confirms that oleic acid successfully covers the GNPs' surface.

The coverage and bonding nature of oleic acid on the GNPs' surface were investigated using FTIR spectroscopy. Illustrated in Figure 3 is the FTIR spectrum of the oleic-modified GNPs material. It can be obvious that the characteristic absorption bands of the GNPs at 3424 (OH $^-$ ), 1629 (OH $^-$ ), 2369 (COO $^-$ ), and 1055  $\text{cm}^{-1}$  (C–O) are hardly observed in the FTIR spectrum, which is ascribed to the uniform coverage of oleic acid on the GNPs' surface. The symmetric and asymmetric vibrations of  $-\text{CH}_2$  stretching in the alkyl chain of oleic acid are clearly observed at 2926 and 2855  $\text{cm}^{-1}$ , respectively. The sharp absorption peaks at 1710 and 1285  $\text{cm}^{-1}$  are assigned to the carboxylic group's C=O and C–O stretching vibrations, respec-

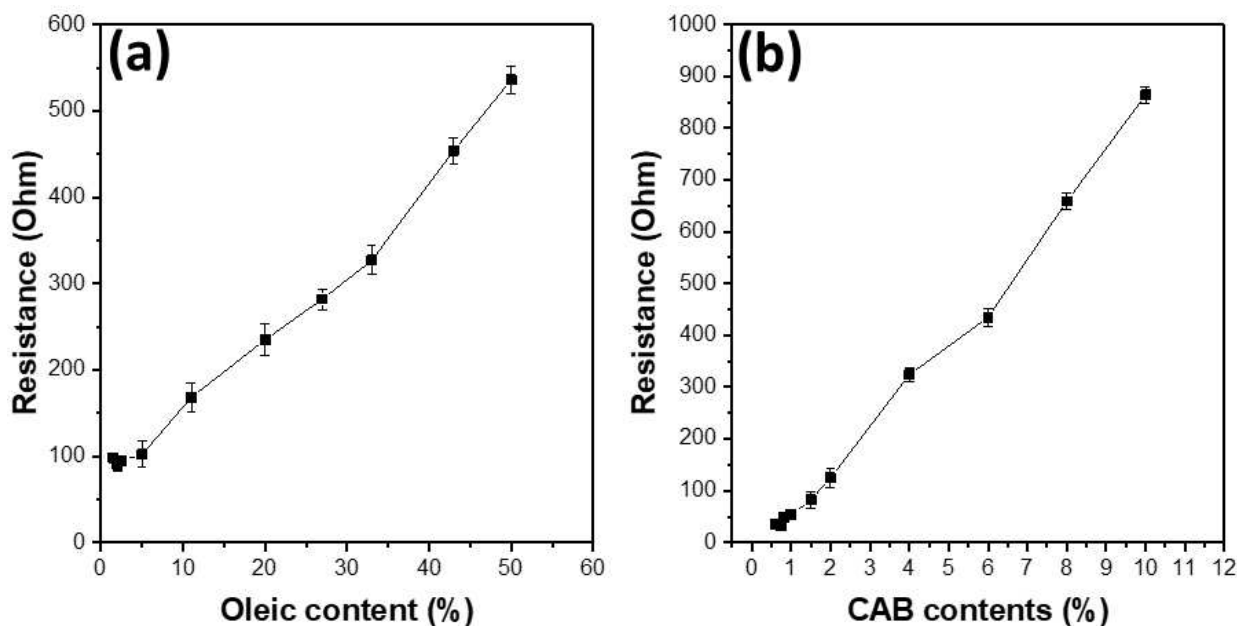


Figure 4. The effect of oleic content (a) and CAB content (b) on the resistivity of the modified GNPs conductive ink.

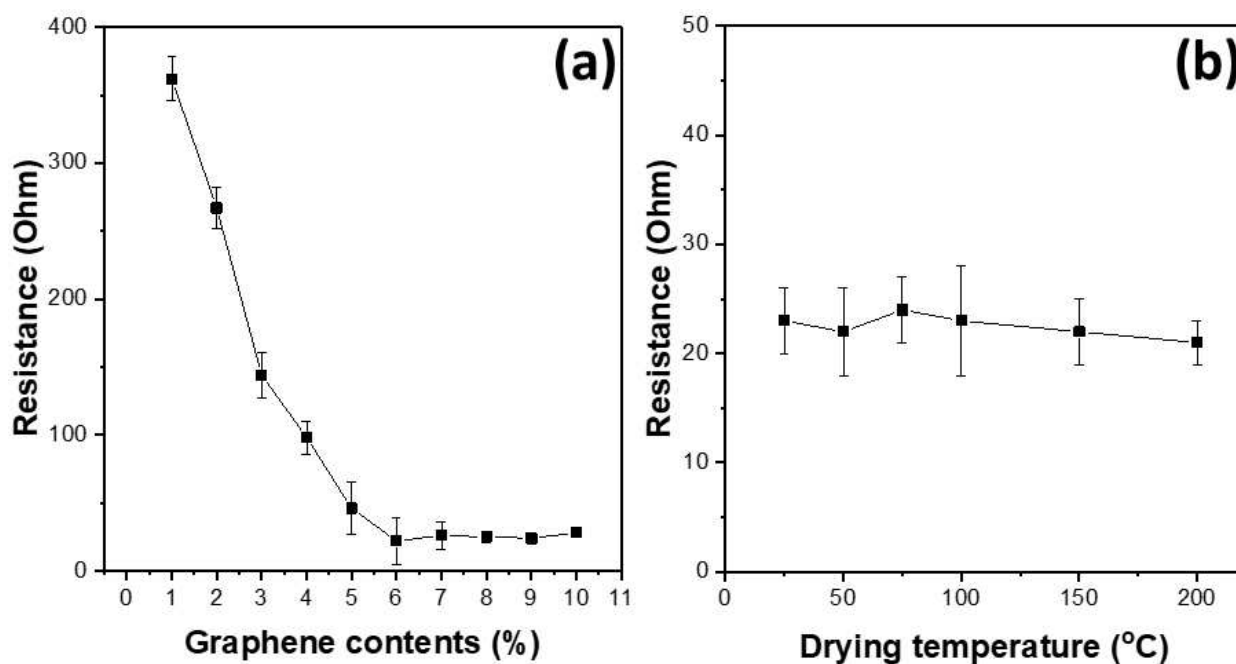
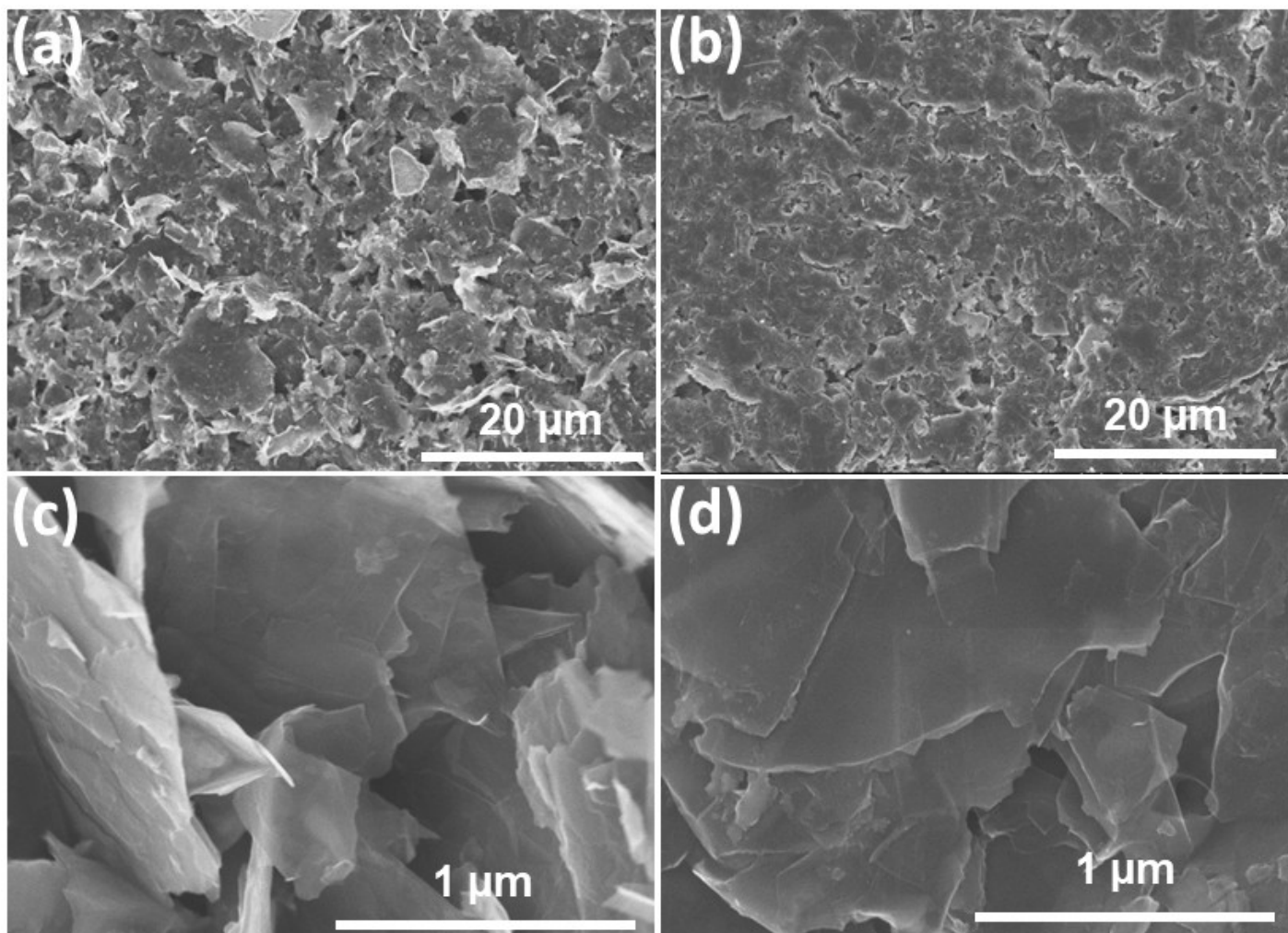


Figure 5. The effect of the modified GNPs content (a) and drying temperature (b) on the conductivity of the modified GNPs-based ink.

tively. The band at  $1461\text{ cm}^{-1}$  is attributed to the bending vibration of ( $\text{CH}_2$ ). This result confirms that the entire surface of the GNPs was evenly covered by oleic acid. The bonding between the GNPs and the oleic acid is probably due to  $\pi$ - $\pi$  interactions. The BET surface area of the graphene nanoplatelets was determined to be approximately  $1045\text{ m}^2/\text{g}$  (Figure S3), which is relatively high for the fabrication of conductive inks.

The concentrations of the modified GNPs, oleic acid, and CAB adhesive in the ink formula greatly affect the conductivity of the resultant conductive ink. Figure 4a shows the effect of the oleic acid's contents on the resistivity of the modified GNPs conductive ink on the paper's surface with the ink's formula of 1.5% CAB binder and 4% modified GNPs. The resistivity is in inverse relation with the conductivity; the lower resistivity means higher conductivity. The resistivity of graphene con-





**Figure 6.** The SEM images of the modified GNPs conductive ink on the paper before (a,c) and (b,d) after pressing.

ductive ink decreases gradually as the oleic content decreases. At the oleic acid content of 50%, the resistance of the ink is determined to be approximately 546  $\Omega$ .cm. When oleic acid content decreases, the resistivity of the ink significantly declines to 100  $\Omega$ .cm at the oleic acid content of 2.5%. This could be explained by the oleic acid's non-conductive nature of the oleic acid, thus when oleic acid increases, the conductivity decreases. Further decrease of the oleic acid content to less than 2.5%, the conductivity decrease because of the low dispensability of the modified GNPs in the ink formula. Thus, 2.5% was selected to be optimal oleic acid content used for modifying GNPs in the formula of modified GNPs conductive ink.

The CAB binder plays a significant role in the adhesion of the ink on the substrates and greatly affects the ink's conductivity. Figure 4b exhibits the effect of the CAB binder content on the resistivity of the modified GNPs conductive ink. In general, the conductivity of the ink increases along with the CAB binder content. With 10% of the CAB in the ink's formula, the resistance of the ink on the substrate is determined to be

about 864  $\Omega$ .cm. The ink's resistance decreases quickly when the CAB binder contents decrease. Similar to oleic acid, the decrease in the ink's resistance and the decrease of the CAB content are ascribed to the non-conductive nature of the CAB organic compound. At the CAB content of 0.75%, the ink's resistance is measured to be only 32  $\Omega$ .cm. Interestingly, when the CAB content decreases to lower than 0.75%, the resistivity of the ink starts to increase. This increase in the ink's resistance is due to the low adhesion of the ink on the substrate as well as between other components in the ink's formula. Thus, the optimal CAB binder content is selected to be 0.75%.

The main conductive component in the ink's formula is the modified GNPs. Thus, the GNPs concentration in the ink's formula is one of the decisive factors affecting the conductivity of the resultant ink. Because of the highly conductive nature of the GNPs, it is reasonable that the increase of the GNPs' content will improve the conductivity of the resultant ink. Illustrated in Figure 5 is the effect of the modified GNPs content on the resistivity of the conductive ink prepared with 0.75% CAB binder. It can be seen that the ink's resistance sharply

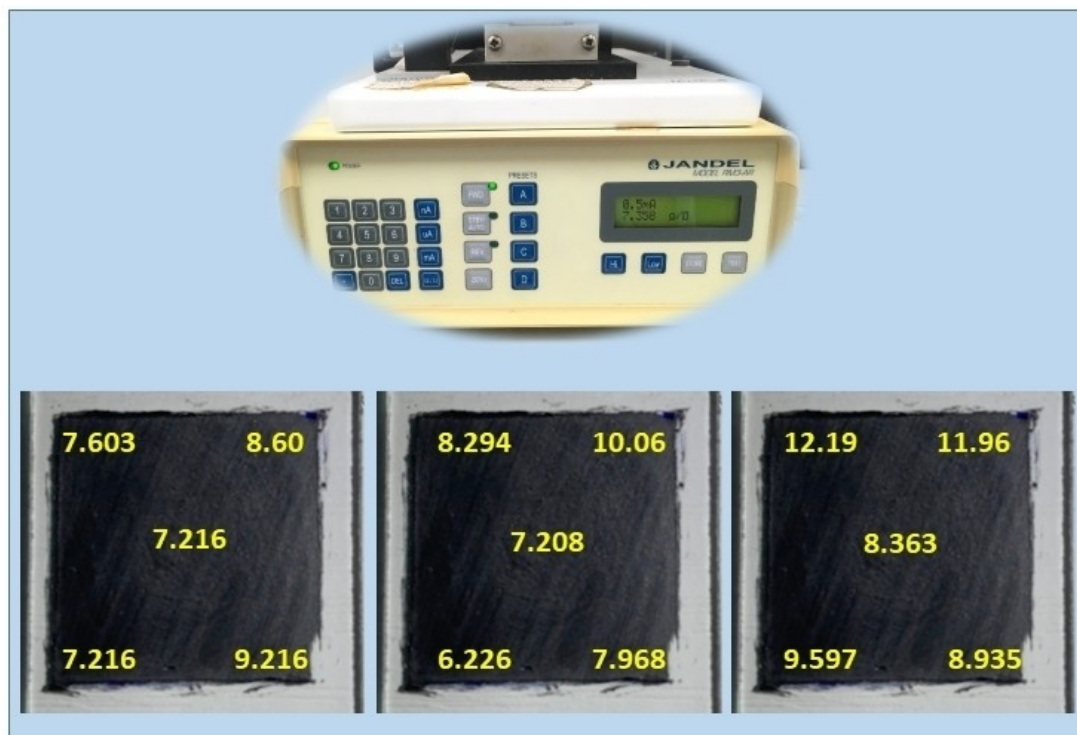


Figure 7. Four-probe resistance measurement of the modified GNPs-based conductive ink.

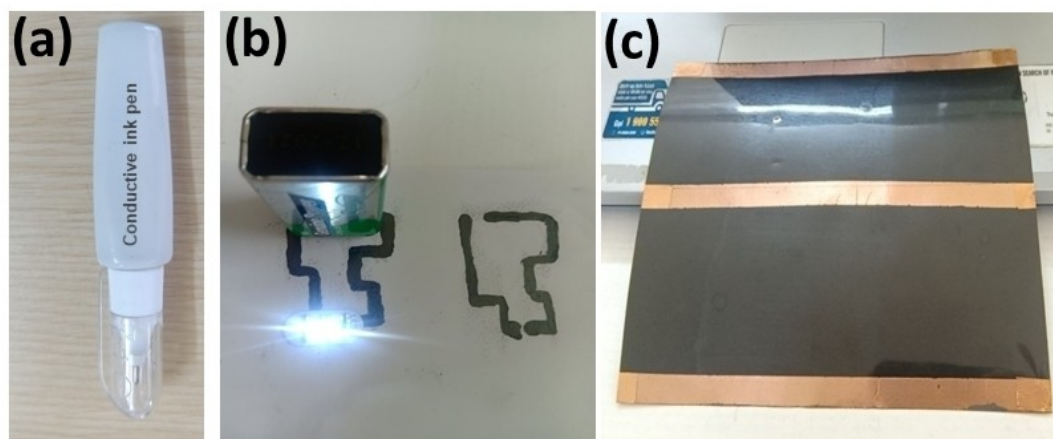


Figure 8. (a) The modified GNPs conductive ink pen, (b) simple electrical circuit on the paper, and (c) the modified GNPs conductive ink on copper foil.

decreases from about 360  $\Omega\cdot\text{cm}$  at 1% modified GNPs to only 22  $\Omega\cdot\text{cm}$  at 6% modified GNPs. However, when the modified GNPs content was increased to higher than 6%, the resistance of the ink increases slightly due to the increase in the ink's viscosity and lack of binder to join the modified GNPs to each other. Thus, the modified GNPs content of 6% is chosen to be the optimal proportion of GNPs in the ink's formula.

For the practical application of the conductive ink, the drying temperature of the ink after applying to the substrate is essential. Therefore, in this work, the effect of the drying temperature on the conductivity of the modified GNPs-based

ink prepared from 0.75% CAB binder and 6% modified GNPs; the result is shown in Figure 5b. It can be seen that the drying temperature negligibly affects the conductivity of the ink, indicating that the modified GNPs-based conductive ink could be employed for the flexible electronics devices processing at room temperature.

The morphology of the modified GNPs-based conductive ink printed on the paper substrate was investigated using scanning electron microscopy, as shown in Figure 6. Figure 6a shows the SEM image of the graphene ink printed in the paper substrate dried at room temperature before pressing by a two-

roller machine. The modified GNPs flakes can be observed in the ink formulation. The thick and dense GNPs flakes are ascribed to the stack of the GNPs by the CAB binder. After pressing, the ink's surface becomes much smoother, enabling more contact between the modified GNPs flakes; as a result, the conductivity of the ink significantly improves. The modified GNPs conductive ink resistance was measured to be about 74  $\Omega\cdot\text{cm}$  before pressing. However, after pressing by a two-roller machine, the resistance decreases to only 22  $\Omega\cdot\text{cm}$ . Thus, the pressing technique is utilized to improve the conductivity of the GNPs-based ink in practical application.

The sheet resistivity of the modified GNPs-based conductive ink was determined using four-probe resistance measurements for thin films. The modified GNPs ink was printed on 2×2 cm glass, dried at room temperature, followed by pressing with a two-roller machine. The results are shown in Figure 7. The average resistivity value is 7.56  $\Omega\cdot\text{cm}^2$ , indicating that the modified GNPs-based ink is of substantially electrical conductivity for electronics and sensing applications.<sup>[45,46]</sup>

The viscosity of the modified GNPs conductive ink prepared with 0.75% CAB binder and 6% GNPs (modified with 2.5% oleic acid) could be facily controlled by adjusting the amount of solvent. Depending on the viscosity, the prepared conductive could be used in pen, painting, or inkjet printing to draw or print on a range of substrates such as paper, plastic, glass, metals, woods, and fabric. A typical conductive ink fabricated from the modified GNPs-based ink is shown in Figure 8a. The conductive ink pen was employed to draw a simple circuit on the paper substrate, as shown in Figure 8b. When a battery source was applied to one end of the circuit, the led light brightened immediately at the other end of the circuit, demonstrating that the modified-GNPs ink is highly conductive. The prepared ink could also be inkjet-printed on a range of substrates. Figure 8c reveals inkjet printing typical ink film on the copper foil's surface. The ink film on the copper foil is uniform, smooth, and durable without and crack after bending the foil to nearly 90°. These applications and results indicate that the modified GNPs conductive ink is highly promising for application in flexible electronic devices and sensing.

## Conclusions

In short, the graphene nanoplatelets have been successfully modified with oleic acid to improve the dispensability in organic solvents. The modified GNPs was utilized as the main component to fabricate the conductive ink sintering at low temperature. The effects of the oleic acid, CAB binder, GNPs contents, and drying temperature on the conductive of the resultant ink were investigated in detail. The optimal composition of the conductive ink was drawn with 0.75% CAB and 6% GNPs (modified with 2.5% oleic acid). The prepared GNPs conductive ink could be fully aged at room temperature with line resistance of 22  $\Omega\cdot\text{cm}$  and sheet resistance of 7.56  $\Omega\cdot\text{cm}^2$ . By adjusting the viscosity of the conductive ink using solvents, the ink could be facily applied to many substrates by pen, painting, or inkjet printing. With high conductivity, process-

ability, low-temperature processing, and durability, the modified GNPs conductive ink is promising for many applications in practice, such as flexible electronic devices and sensing.

## Supporting information summary

This provides further information about the experimental section, EDX spectrum, AFM image, and BET surface area plot of the graphene nanoplatelets.

## Conflict of Interest

There are no conflicts of interest

## Data Availability Statement

The data that support the findings of this study are available in the supplementary material of this article.

**Keywords:** Graphene · conductive ink · nanotechnology · flexible electronic devices

- [1] V. Wood, M. J. Panzer, J. Chen, M. S. Bradley, J. E. Halpert, M. G. Bawendi, V. Bulović, *Adv. Mater.* **2009**, *21*, 2151–2155.
- [2] W. Shen, X. Zhang, Q. Huang, Q. Xu, W. Song, *Nanoscale*. **2014**, *6*, 1622–1628.
- [3] R. Liu, F. Shen, H. Ding, J. Lin, W. Gu, Z. Cui, T. Zhang, *J. Micromech. Microeng.* **2013**, *23*, 065027.
- [4] M. Singh, H. M. Haverinen, P. Dhagat, G. E. Jabbour, *Adv. Mater.* **2010**, *22*, 673–685.
- [5] O.-S. Kwon, H. Kim, H. Ko, J. Lee, B. Lee, C.-H. Jung, J.-H. Choi, K. Shin, *Carbon*. **2013**, *58*, 116–127.
- [6] Y. Feng, J. Li, R. Tian, J. Yao, *J. Energy Chem.* **2021**, *53*, 433–440.
- [7] N. Zavanelli, W.-H. Yeo, *ACS Omega*. **2021**, *6*, 9344–9351.
- [8] S. Jeong, H. C. Song, W. W. Lee, S. S. Lee, Y. Choi, Y. W. Son, E. D. Kim, C. H. Paik, S. H. Oh, B.-H. Ryu, *Langmuir*. **2011**, *27*, 3144–3149.
- [9] L. Hu, M. Pasta, F. La Mantia, L. Cui, S. Jeong, H. D. Deshazer, J. W. Choi, S. M. Han, Yi Cui, *Nano Lett.* **2010**, *10*, 708–714.
- [10] Y.-L. Tai, Z.-G. Yang, *J. Mater. Chem.* **2011**, *21*, 5938–5943.
- [11] A. Russo, B. Y. Ahn, J. J. Adams, E. B. Duos, J. T. Bernhard, J. A. Lewis, *Adv. Mater.* **2011**, *23*, 3426–3430.
- [12] W. R. Small, M. in het Panhuis, *Small*. **2007**, *3*, 1500–1503.
- [13] N. Perinka, C. H. Kim, M. Kaplanova, Y. Bonnassieux, *Phys. Procedia*. **2013**, *44*, 120–129.
- [14] S. Magdassi, M. Grouchko, O. Berezin, A. Kamysny, *ACS Nano*. **2010**, *4*, 1943–1948.
- [15] R. Shankar, L. Groven, A. Amert, K. W. Whites, J. J. Kellar, *J. Mater. Chem.* **2011**, *21*, 10871–10877.
- [16] W.-d. Yang, C.-y. Liu, Z.-y. Zhang, Y. Liu, S.-d. Nie, *J. Mater. Chem.* **2012**, *22*, 23012–23016.
- [17] Q. Huang, Y. Zhu, *Adv. Mater.* **2019**, *4*, 1800546.
- [18] X. Wu, Z. Zhou, Y. Wang, J. Li, *Coating* **2020**, *10*, 865.
- [19] J. Perelaer, B. J. De Gans, U. S. Schubert, *Adv. Mater.* **2006**, *18*, 2101–2104.
- [20] P. Smith, D.-Y. Shin, J. Stringer, B. Derby, N. Reis, *J. Mater. Sci.* **2006**, *41*, 4153–4158.
- [21] B. K. Park, D. Kim, S. Jeong, J. Moon, J. S. Kim, *Thin Solid Films*. **2007**, *515*, 7706–7711.
- [22] D.-H. Shin, S. Woo, H. Yem, M. Cha, S. Cho, M. Kang, S. Jeong, Y. Kim, K. Kang, Y. Piao, *ACS Appl. Mater. Interfaces*. **2014**, *6*, 3312–3319.
- [23] Y. Farraj, M. Grouchko, S. Magdassi, *Chem. Commun.* **2015**, *51*, 1587–1590.
- [24] D. Saidina, N. Eawwiboonthanakit, M. Mariotti, S. Fontana, C. Hérold, *J. Electronic Mater.* **2019**, *48*, 3428–3450.
- [25] Y. Htwe, M. Abdullah, M. Mariotti, *Syn. Metals*. **2021**, *274*, 116719.

- [26] Z. Fan, W. Tong, G. Luo, F. Wei, *J. Mater. Sci.* **2005**, *40*, 5075–5077.
- [27] A. Aziz, M. B. Bazbouz, M. E. Welland, *ACS Appl. Nano. Mater.* **2020**, *3*, 9385–9392.
- [28] R. P. Tortorich, J.-W. Choi, *Nanomaterials*. **2013**, *3*, 453–468.
- [29] K. Kordás, T. Mustonen, G. Tóth, H. Jantunen, M. Lajunen, C. Soldano, S. Talapatra, S. Kar, R. Vajtai, P. M. Ajayan, *Small*. **2006**, *2*, 1021–1025.
- [30] A. K. Geim, *Science*. **2009**, *324*, 1530–1534.
- [31] M. D. Stoller, S. Park, Y. Zhu, J. An, R. S. Ruoff, *Nano Lett.* **2008**, *8*, 3498–3502.
- [32] D. D. La, A. Rananaware, M. Salimimarand, S. V. Bhosale, *ChemistrySelect*. **2016**, *1*, 4430–4434.
- [33] D. D. La, H. P. N. Thi, T. A. Nguyen, S. V. Bhosale, *New J. Chem.* **2017**, *41*, 14627–14634.
- [34] D. D. La, T. N. Truong, T. Q. Pham, H. T. Vo, T. A. Nguyen, A. K. Nadda, T. T. Nguyen, S. W. Chang, W. J. Chung, D. D. Nguyen, *Nanomaterials*. **2020**, *10*, 877.
- [35] M. D. D. La, S. Bhargava, S. V. Bhosale, *ChemistrySelect* **2016**, *1*, 949–952.
- [36] W. Yang, C. Wang, *J. Mater. Chem. C*. **2016**, *4*, 7193–7207.
- [37] L. Huang, Y. Huang, J. Liang, X. Wan, Y. Chen, *Nano Res.* **2011**, *4*, 675–684.
- [38] F. Torrisi, T. Hasan, W. Wu, Z. Sun, A. Lombardo, T. S. Kulmala, G.-W. Hsieh, S. Jung, F. Bonaccorso, P. J. Paul, D. Chu, A. C. Ferrari, *ACS Nano*. **2012**, *6*, 2992–3006.
- [39] M. Mathesh, J. Liu, N. D. Nam, S. K. H. Lam, R. Zheng, C. J. Barrow, W. Yang, *J. Mater. Chem. C* **2013**, *1*, 1–7.
- [40] Y. Gao, W. Shi, W. Wang, Y. Leng, Y. Zhao, *Ind. Eng. Chem. Res.* **2014**, *53*, 16777–16784.
- [41] A. Zhang, T. Chen, S. Song, W. Yang, J. J. Gooding, J. Liu, *J. Colloid Interface Sci.* **2021**, *594*, 460–465.
- [42] L. Liao, D. Jiang, K. Zheng, M. Zhang, J. Liu, *Advanced Functional Materials* **2021**, *31*, 2103960.
- [43] J. Liu, J. Tang, J. J. Gooding, *J. Mater. Chem.* **2012**, *22*, 12435–12452.
- [44] S. P. Lonkar, Y. S. Deshmukh, A. A. Abdala, *Nano Res.* **2015**, *8*, 1039–1074.
- [45] K. Arapov, R. Abbel, G. de With, H. Friedrich, *Faraday Discuss.* **2014**, *173*, 323–336.
- [46] A. Capasso, A. D. R. Castillo, H. Sun, A. Ansaldo, V. Pellegrini, F. Bonaccorso, *Solid State Commun.* **2015**, *224*, 53–63.

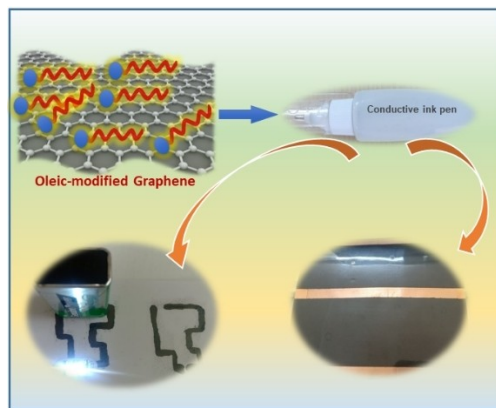
Submitted: November 29, 2021

Accepted: December 29, 2021



## RESEARCH ARTICLE

---



*Dr. T. T. Le, H. H. T. Bui, A. K. P. Dinh,  
D. V. Van, Dr. Q. D. Ho, H. A. N. Thi,  
Prof. D. H. Nguyen, Dr. D. D. La\**

1 – 9

**Room Temperature-Sintering Conductive Ink Fabricated from Oleic-Modified Graphene for the Flexible Electronic Devices**



The graphene nanoplatelets were successfully modified with oleic acid to improve their dispersability in organic solvents. The modified GNPs were utilized as a main component fabrication of room temperature-sintering conductive ink. The effects of the oleic acid, CAB binder, GNPs contents, and drying temperature on the con-

ductivity of the ink were investigated in detail. The optimized compositions of the conductive ink was drawn with 0.75% CAB and 6% GNPs (modified with 2.5% oleic acid). The prepared GNPs conductive ink could be fully aged at room temperature with line resistance of 22  $\Omega$ .cm and sheet resistance of 7.56  $\Omega$  cm<sup>2</sup>.

---